

Learning to Navigate from Scratch using World Models and Curiosity: the Good, the Bad, and the Ugly

Daria de Tinguy^{*1}, Sven Remmery^{*1}, Pietro Mazzaglia¹, Tim Verbelen² and Bart Dhoedt¹

Abstract—Learning to navigate unknown environments from scratch is a challenging problem. This work presents a system that integrates world models with curiosity-driven exploration for autonomous navigation in new environments. We evaluate performance through simulations and real-world experiments of varying scales and complexities. In simulated environments, the approach rapidly and comprehensively explores the surroundings. Real-world scenarios introduce additional challenges. Despite demonstrating promise in a small controlled environment, we acknowledge that larger and dynamic environments can pose challenges for the current system. Our analysis emphasizes the significance of developing adaptable and robust world models that can handle environmental changes to prevent repetitive exploration of the same areas.

I. INTRODUCTION

Navigation is an extensively studied domain within the field of robotics, where classical solutions typically combine mapping and planning routines. Traditional approaches involve space representation in grid [1], [2] and/or topological maps [3], [4] based on observed data, over which motion planning algorithms are employed to guide robots through the environment. However, the efficacy of these approaches is inevitably intertwined with the critical hurdle of exploration.

Exploration, as a crucial part of navigation, is a puzzle. Uncovering new regions, detecting obstacles, and deducing viable approaches, all while learning a sensible model of the environment, are all part of the process. In light of these challenges, recent research has shed light on the integration of machine learning techniques to augment the autonomy and adaptability of models, enabling them to adeptly navigate uncharted scenarios [5], [6].

The combination of world models with reinforcement learning (RL) [7], [8], [9], [10] has emerged as a powerful data-driven strategy for enhancing decision-making prowess within real-world contexts [11], [12]. However, it is worth noting that the application of this approach to real-world scenarios has predominantly centered around constrained workspaces, such as manipulation tasks [13], [14], [15], [16], [17], or locomotion endeavors [18], [19], [20].

This work proposes and evaluates a machine learning system for learning robotic navigation from scratch, using world models, for learning a representation of the environment, model-based RL, to drive low-level actions, and curiosity-driven exploration, to discover reachable areas in the environment. We aim to analyze whether current trends

in machine learning, such as world models and unsupervised RL, already constitute valuable means for real-world robotic navigation, from simulation to real-world applications of diverse scale and complexity.

Contributions. Our work can be summarized as follows:

- We present a system that combines world models for learning actions [21] with curiosity-driven exploration [22] (Section III).
- We evaluate the system in simulation using the Habitat navigation environment [23]. Our method outperforms previous state-of-the-art approaches [24] when comparing the percentage of the environment explored (*the good*, Section IV-A).
- We design a remote-computing pipeline to apply our system in real-world scenarios and evaluate it in two environments: a controlled small-scale environment, where the agent performs well, and an uncontrolled experiment in a larger-scale environment, where the agent’s exploration capabilities are impaired (*the bad*, Section IV-B).
- We quantitatively and qualitatively assess our work, demonstrating how the generative world model underperforms when visual aspects of the environment change during training (e.g. objects are rearranged in a room). We observe that the agent’s imagined trajectories struggle to match the dynamism of reality (*the ugly*, Section IV-C).

Overall, our system demonstrates high autonomous exploration performance in simulated and small-scale real-world environments. However, in a larger environment, the agent’s performance is hindered by hardware and model limitations, resulting in a limited exploration. We hope that this investigation will drive further developments in this promising research direction.

II. RELATED WORK

Robot navigation. Robotic navigation has been a long-standing challenge, often involving simultaneous localization and mapping (SLAM) techniques. Traditional methods typically focus on building metric (grid) [1], [2], topological [3] or both maps [4] of the environment and then use motion planning algorithms to navigate through it. Despite the progress made, it is acknowledged that these approaches lack autonomy in complex environments [25]. For example, active SLAM struggles with challenges like predicting robot localization uncertainty, creating semantic-like mappings, and reasoning in dynamic and changing spaces [5], [6].

^{*}Equal contribution

¹Department of Information Technology, University of Ghent, Ghent, Belgium, ²Verses AI, Vancouver, Canada {Correspondence to: Daria de Tinguy <Daria.detinguy at ugent.be>}

Recent research has sought to enhance robotic navigation with machine learning techniques, aiming to imbue models with adaptability and autonomy in new scenarios. Different approaches have been explored to address navigational challenges by acquiring navigational skills from simulation [26], [27], human-provided labels [28], [29], human demonstration [30] or through lifelong learning [24], [31], [32].

World models. World models have gained traction alongside reinforcement learning (RL) approaches, as they provide the agent with an internal representation of the environment. These models allow agents to simulate and plan future trajectories, thereby supporting decision-making and adaptability [33]. Combining world models with RL for decision-making enables solving tasks driven by a reward function [7], [21] and has shown benefits in terms of data-efficiency for real-world problems as well [11], [12], [34]. However, notable works combining RL and world models in real-world environments have predominantly focused on specific contexts such as arm manipulation [13], [14], [15], [16], [17] or locomotion control [18], [19], [20].

Exploration. Extensive literature exists in the context of unsupervised exploration and unsupervised objectives for control [22], [35], [36], [37], [38], [39], [24], with some of these works also combining exploration with world models applied in simulated manipulation and locomotion environments [40], [41]. Only a few studies combine world models and RL for navigation, and even fewer propose an exploration behavior not relying on a goal objective to stimulate exploration. The approach described in Nozari & al. [8] proposes a generative model aiming to enhance both exploratory and exploitative navigation in unexpected situations without necessarily relying on goal objectives. Wu & al. work [9] centers on the maximization of mutual information between actions and subsequent observations to facilitate objective-driven navigation, in order to reach an objective. It’s worth noting, however, that both of these approaches necessitate expert data for training. The RECON system [10] introduces a strategy enabling exploration and navigation in open-world environments. It is achieved through the utilization of learned goal-conditioned distance models and latent variables that represent visual objectives. The approach fosters goal-directed exploration and is fine-tuned via real-world trial and error.

III. METHOD

Our approach combines two popular trends in reinforcement learning and aims to study them for robotic navigation: world models, and unsupervised exploration.

Setting. The control setting for navigation can be formalized as a Partially Observable Markov Decision Process (POMDP) operating at a discrete frequency, for which we use subscripts to indicate the timesteps. In the POMDP, observations x_t are generated at each timestep, based on the internal hidden state of the environment. Actions a_t enable interaction between the agent and the environment. In this work, we use RGB images as observations while actions are

the robot’s discrete spatial displacements, with respect to its position.

A. World model

To address the challenges posed by the POMDP, where the agent cannot observe the hidden state of the environment, we adopt a world model using a recurrent state-space model (RSSM) [42] for the dynamics. This allows learning an internal representation of model states s_t that summarizes and reflects the environment dynamics, integrating knowledge over sequences of observations and actions, thanks to the recurrent memory module.

The world model is composed of the following components:

$$\begin{aligned} \text{Posterior: } & q_\phi(s_t | s_{t-1}, a_{t-1}, x_t), \\ \text{Dynamics: } & p_\phi(s_t | s_{t-1}, a_{t-1}), \\ \text{Decoder: } & p_\phi(x_t | s_t). \end{aligned}$$

The model states s_t have both a deterministic component, modeled using the RSSM [42], and a discrete stochastic component [21], capturing the uncertainty of the dynamics. The remaining modules are CNNs [43], given the high-dimensionality (pixel-based observations) of the input. The model is trained end-to-end by optimizing the evidence lower bound (ELBO) on the log-likelihood of data:

$$\begin{aligned} \mathcal{L}_{\text{wm}} = & D_{\text{KL}}[q_\phi(s_t | s_{t-1}, a_{t-1}, x_t) || p_\phi(s_t | s_{t-1}, a_{t-1})] \\ & - \mathbb{E}_{q_\phi(s_t)}[\log p_\phi(x_t | s_t)], \end{aligned} \quad (1)$$

where sequences of observations x_t and actions a_t are sampled from a replay buffer, that is collected online by the agent through exploration.

Leveraging this generative world model, the agent can engage in simulated scenarios to explore potential actions and their consequences. This imaginative environment allows the agent to learn and refine its decision-making policies through interactions without directly impacting the real-world environment. Combined with RL techniques [21], [7], this mechanism enables data-efficient learning of behavior policies “in imagination”.

B. Exploration

For exploring the space to navigate, we are interested in collecting data that is informative about new areas of the environment. Inspired by curiosity-driven approaches [22], [38], [35], we would like to measure the amount of information that is gained by the model when facing a new environment’s transition and use that as an intrinsic reward to foster exploration in RL, using the world model. Every time the agent takes action a_t while being in the internal state s_t , it moves from time t to $t + 1$, therefore receiving a new observation x_{t+1} from the environment, that will make the internal state transition to s_{t+1} .

Following [22], the information gained by the world model with the transition can be approximated using the KL divergence between the latent posterior and dynamics and

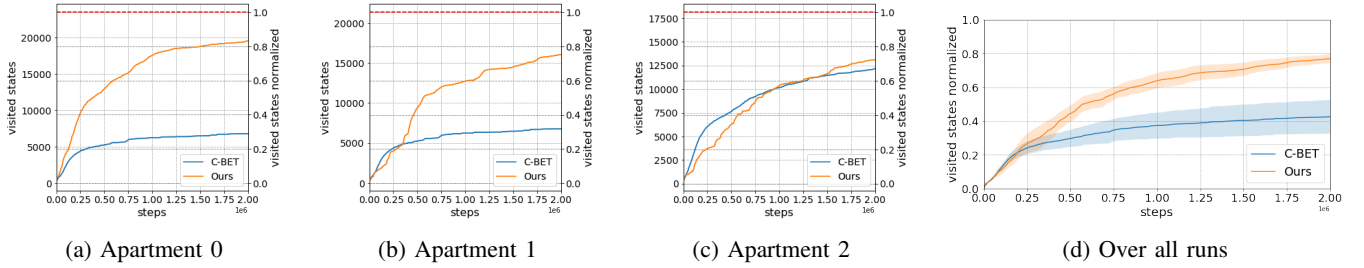


Fig. 1: C-BET and our agent’s performance comparison over 3 Habitat environments. For each figure, on the left, the number of visitable states the agents reached, the dotted line representing the environment maximum visitable states. On the right, the coverage percentage the agent reached. (d) shows the mean of the normalized visited states over all the environments.

adopted as an intrinsic reward for RL as follows:

$$r_{\text{expl}} = \mathcal{I}(s_{t+1}; x_{t+1} | s_t, a_t) \approx D_{\text{KL}}[q_\theta(s_{t+1} | s_t, a_t, x_{t+1}) || p_\theta(s_{t+1} | s_t, a_t)] \quad (2)$$

The above term can be efficiently computed by comparing the distributions predicted by the latent dynamics and the latent posterior components. The signal provided should encourage the agent to collect transitions where the predictions are more uncertain or erroneous.

In order to leverage the world model for learning actions, we train the exploration actor and critic networks in imagination [21], to maximize the expected reward presented in Equation 2. Actor and critic networks are implemented as MLP and defined as follows:

$$\begin{aligned} \text{Expl. actor: } & \pi_{\text{expl}}(a_t | s_t), \\ \text{Expl. critic: } & v_{\text{expl}}(s_t), \end{aligned} \quad (3)$$

Please refer to the Appendix A for the hyperparameters of the world model and the exploration actor-critic.

C. Lifelong learning

All agents are trained in an episodic setting. In each episode, the agent interacts N steps with the environment, storing its actions and observations in a replay buffer. Next, we train the model for K iterations on the replay buffer data and update the agent’s world model and policies with the new parameters. Finally, the agent is respawned at the starting position, and a new episode starts.

In the real world, we cannot respawn the agent automatically. In this case, the starting position is defined as the charging station, and we command the robot to return to the charging station at the end of the episode. To enable this, we set up a navigation stack that fuses odometry, IMU and LiDAR data through an Extended Kalman Filter (EKF) [44] enabling the robot to be guided back to the charging station. More information about the auto docking strategy can be found in Appendix D. Each time the agent docks, the latest episode is sent to a local cloud storage and we execute the model train iterations on a GPU server, using a GTX 1080.

In our experiments, we used $N = 500$ steps as episode length, and $K = 100$ for updating the models between episodes, sampling sequences of steps over all the collected episodes.

IV. EXPERIMENTAL RESULTS

Our experiments are designed to highlight the agent’s ability to explore a totally new environment, using only visual observations and low-level actions.

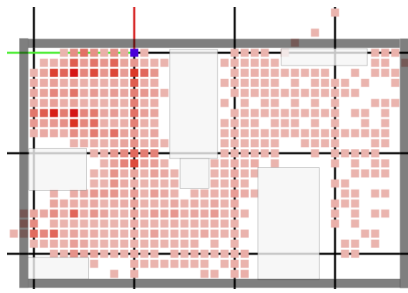
Environments. The experiments are divided into two main groups. The first group is realized on Habitat [23], a navigation simulator showcasing a visually realistic domain. The second group studies real environments of diverse size and complexity. Consistently across all environments, the tests are realized with the limited field of view of a single camera seeing in front of the agent (i.e egocentric view). Each state corresponds to a visual observation and each observation corresponds to the agent first view 64×64 RGB image. The agent moves in discrete steps in the environment, each step corresponding to a motion forward (0.25m) or a turn right or left (10°).

A. Simulation

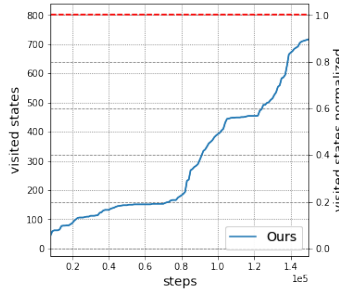
To establish a baseline for the Habitat simulation tasks, we utilize C-BET, an exploration approach that seek out both surprising and high-impact areas of the environment, and that has been shown to perform well on this benchmark [24]. Both our proposed model and C-BET aim to fully explore the environment by physically cover visitable states, which are represented as plan cells of 5×5 cm in the Habitat simulations. We conduct exploration experiments in three diverse apartments of $52,43\text{m}^2$ averaged surface, as presented in Appendix B. Results show that our agent outperforms C-BET in terms of exploration coverage and efficiency, as illustrated in Fig. 1 for individual apartments (1a,1b,1c), as well as the overall mean results across all environments (1d).

B. Real world

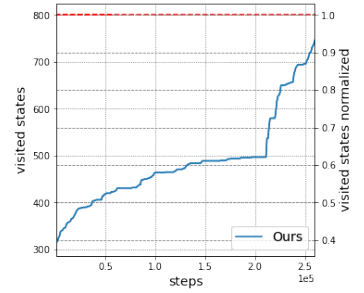
Setup. In our real-world experiments, we employ a Kobuki TurtleBot 2i as the platform, with a Jetson AGX Orin serving as the core system. Data from the robot is sent to a computer for training after each episode, and an Intel Realsense LiDAR Camera L515 is utilized to perceive RGB and depth information, with depth data specifically used for obstacle detection and avoidance, cancelling any forward motion leading to a collision. The Robot Operating System (ROS), a framework to help build and control robots, providing tools and libraries for tasks such as communication, hardware control, and



(a) Coverage heatmap.



(b) Run 1



(c) Run 2

Fig. 2: (a) Coverage heatmap of the environment with a coarse positioning of the obstacles. Blue square is the starting position. We can see that Run 1 (b) outperforms Run 2 (c), as in the latter the agent discovers the furthest area only after 250k steps. The blue curve shows the number of visited states covered over the number of total steps, the dotted red line displaying the maximum number of states the environment.

navigation is implemented as the baseline framework for executing the agent’s behavior. In this context, a visitable state in the real world corresponds to a plan cell with dimensions of 10×10 cm.

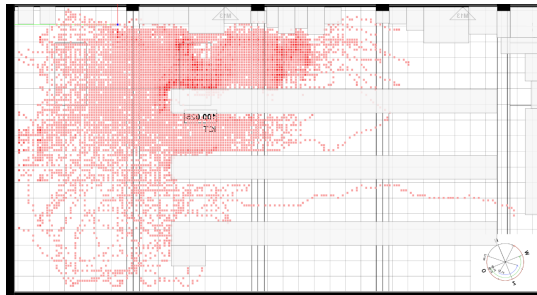
To assess the system’s performance under different conditions, we conducted two tests: one in a small, well-controlled environment, and another in a larger environment with variable conditions and potential changes happening.

Small real-world. The first test composed of 2 runs is conducted in a controlled environment measuring approximately 2×4 square meters. Obstacles are deliberately placed in the environment to introduce complexity and challenges for navigation. It is important to note that during this test, no modifications happen in the environment (lighting or object motion), ensuring a consistent and stable environment throughout the experiment. The agent is able to successfully autonomously navigate and return to its charging station, regardless of the room configuration. In 140k steps, it can achieve a coverage rate of over 80% of the entire environment as displayed in the first run (Fig.2b). The agent follows a pattern of exploration, spending approximately 5 minutes (500 steps) exploring before returning to its docking station. This pattern results in the area around the blue dot in the heat-map (Figure 2a) being more thoroughly explored

compared to the farther areas of the map.

Large real-world. The second environment is significantly more challenging, presenting an environment 4x times larger than in simulation and additional challenges, such as lightning changes and dynamic settings. The large real-world environment covers an area of 10×23 square meters, and presents a more complex environment with various types of obstacles such as similar looking shelves, tables, chairs, and cardboards (see pictures in Appendix C). The lightning is susceptible to change and some obstacles got moved during the exploration phase, adding a significant layer of complexity.

The agent can operate for up to 10 minutes before returning to its charging station due to battery limitations. With this constraint of back and forth, the agent has difficulty exploring the full environment as in simulation. In simulation the agent just resets back to the starting point, in the real world the agent needs to physically return to it, which is to be considered while managing battery level. Fig.3 displays the environment’s coverage of the agent over time and the areas more often visited. The agent starts at the blue square in the heatmap (Fig.3a) and explores thoroughly the vicinity, missing the rest of the environment, reaching a 60% coverage in 600k steps.



(a) Heatmap of the environment coverage. The starting position is highlighted by a blue square.

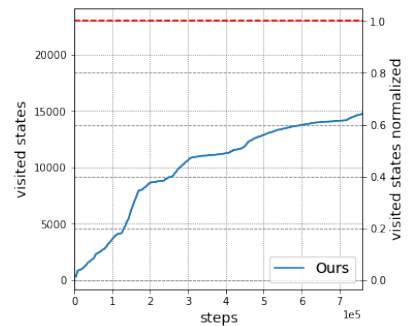


Fig. 3: a) Our model heatmap coverage of the large real world with a coarse positioning of the obstacles. b) the number of visited states over steps coupled with the percentage of the environment it represents.

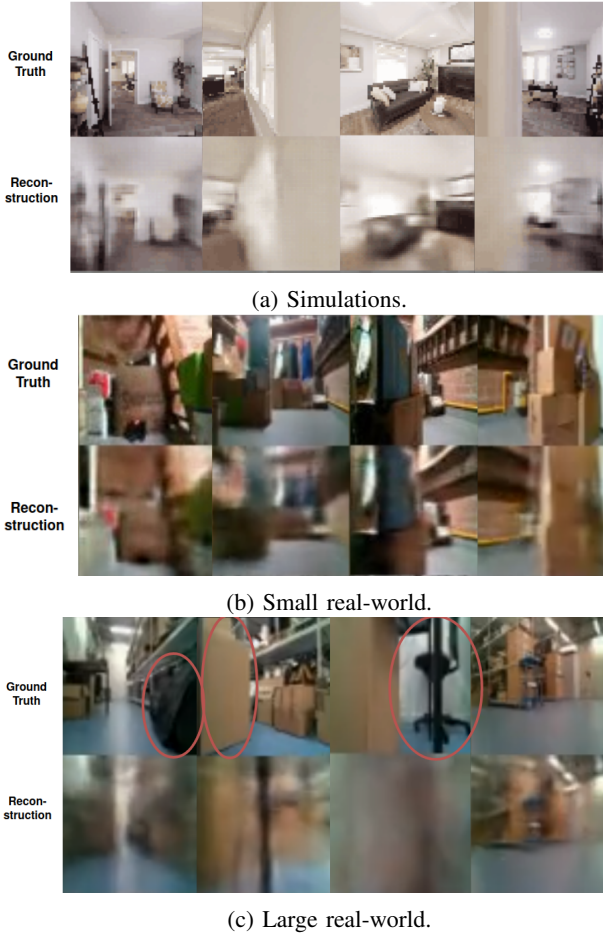


Fig. 4: Randomly selected agent’s observations and their predictions. Top row shows the ground truth, the real observations, bottom row displays the corresponding predictions made by the agent. (c) The discrepancies, corresponding to moved objects are circled in red, those objects (i.e. (cardboard and chair)) are not expected by the agent.

C. Qualitative results

In this section, we delve into the qualitative analysis of our experiments, focusing on the predicted observations generated by the world model. This adds insights into the model’s ability to simulate and understand its environment and helps identifying the current limitations of our system. In Figure 4, we present the agent’s observation predictions (bottom rows) alongside the real observations (top rows), displaying the agent ability to correctly infer the observation a motion should produce.

For the simulations and small real-world experiments, Figure 4a and 4b show that at the end of its training, our agent is able to correctly predict observations. This shows the agent is able to learn a coherent world model of the environment and it explains why the exploration process was efficient and successful.

In the large real-world environment (Fig.4c), the predictions are not always so correctly inferred. When facing changes in the environment, the agent generates different

expectations about what is to be seen considering its position, erroneously perceiving the dynamic state as a new area to explore for the agent. This can be observed in the red-circled areas in the Figure, showing that the agent’s predictions miss the object present in the ground truth images (showing objects that were moved during the exploration process). This shows a major limitation of the current model, not able to adapt for accounting for those object’s motions and consistently predicting erroneous object positions after changes in the environment.

V. CONCLUSION

This work presents a system that merges curiosity-driven exploration with world models to achieve autonomous navigation in both simulated and real-world environments. Our study highlights the challenges of scaling autonomous navigation and exploration, progressing from an analysis in simulation to real-world dynamic and uncontrolled environments. The integration of curiosity-driven exploration and world models aims to enhance the adaptability and autonomy of robotic agents. The experimental results demonstrate improved coverage and exploration speed compared within the Habitat simulation.

Transitioning to real-world experiments, the model performs well in a controlled “small-scale” environment despite hardware limitations. However, exploration in a larger uncontrolled environment reveals the challenges associated with scalability and real-world complexities, including changing lighting conditions and a dynamic environment. While the agent exhibits effective exploration in its vicinity, scalability and adaptability challenges become apparent, with the agent largely revisiting the same areas, and the world model failing to update object positions after displacement.

Our work emphasizes the importance of scalability, robustness, and real-world experimentation in evaluating navigation systems for practical scenarios. While our approach holds promise in controlled settings, addressing the complexities of larger and dynamic environments remains a crucial step toward achieving practical autonomy. The combined approach of world models, curiosity-driven exploration, and reinforcement learning shows potential for enabling autonomous navigation and exploration in diverse and challenging environments. Nonetheless, there are limitations to address, such as the adaptability of the world model, the diminishing efficacy of curiosity-driven exploration in complex and dynamic environments, and the need for adaptation strategies when performing lifelong learning in large-scale environments, which require substantial data for learning about the environment.

ACKNOWLEDGMENT

This research received funding from the Flemish Government (AI Research Program). Pietro Mazzaglia is funded by a Ph.D. grant of the Flanders Research Foundation (FWO).

REFERENCES

- [1] R. Lakaemper, L. J. Latecki, X. Sun, and D. Wolter, "Geometric robot mapping," vol. 3429, 04 2005, pp. 11–22.
- [2] K. Kamarudin, S. M. Mamduh, A. Y. M. Shakaff, and A. Zakaria, "Performance analysis of the microsoft kinect sensor for 2d simultaneous localization and mapping (slam) techniques," *Sensors*, vol. 14, no. 12, pp. 23 365–23 387, 2014. [Online]. Available: <https://www.mdpi.com/1424-8220/14/12/23365>
- [3] S. S. Ge, Q. Zhang, A. T. Abraham, and B. Rebsamen, "Simultaneous path planning and topological mapping (sp2atm) for environment exploration and goal oriented navigation," *Robotics and Autonomous Systems*, vol. 59, no. 3, pp. 228–242, 2011. [Online]. Available: <https://www.sciencedirect.com/science/article/pii/S0921889010002009>
- [4] S.-H. Kim, J.-G. Kim, and T.-K. Yang, "Autonomous slam technique by integrating grid and topology map," in *2008 International Conference on Smart Manufacturing Application*, 2008, pp. 413–418.
- [5] Z. Li, G. Chen, B. Peng, and X. Zhu, "Robot navigation method based on intelligent evolution," in *2018 IEEE 4th Information Technology and Mechatronics Engineering Conference (ITOEC)*, 2018, pp. 620–624.
- [6] S. Levine and D. Shah, "Learning robotic navigation from experience: principles, methods and recent results," *Philosophical Transactions of the Royal Society B: Biological Sciences*, vol. 378, no. 1869, dec 2022.
- [7] D. Hafner, J. Pasukonis, J. Ba, and T. Lillicrap, "Mastering diverse domains through world models," 2023.
- [8] S. Nozari, A. Krayani, P. Marin-Plaza, L. Marcenaro, D. M. Gómez, and C. Regazzoni, "Active inference integrated with imitation learning for autonomous driving," *IEEE Access*, vol. 10, pp. 49 738–49 756, 2022.
- [9] Q. Wu, K. Xu, J. Wang, M. Xu, X. Gong, and D. Manocha, "Reinforcement learning-based visual navigation with information-theoretic regularization," *IEEE Robotics and Automation Letters*, vol. 6, no. 2, pp. 731–738, 2021.
- [10] D. Shah, B. Eysenbach, N. Rhinehart, and S. Levine, "RECON: rapid exploration for open-world navigation with latent goal models," *CoRR*, vol. abs/2104.05859, 2021. [Online]. Available: <https://arxiv.org/abs/2104.05859>
- [11] Y. Matsuo, Y. LeCun, M. Sahani, D. Precup, D. Silver, M. Sugiyama, E. Uchibe, and J. Morimoto, "Deep learning, reinforcement learning, and world models," *Neural Networks*, vol. 152, pp. 267–275, 2022. [Online]. Available: <https://www.sciencedirect.com/science/article/pii/S0893608022001150>
- [12] K. Gregor, D. Jimenez Rezende, F. Besse, Y. Wu, H. Merzic, and A. van den Oord, "Shaping belief states with generative environment models for rl," in *Advances in Neural Information Processing Systems*, H. Wallach, H. Larochelle, A. Beygelzimer, F. d'Alché-Buc, E. Fox, and R. Garnett, Eds., vol. 32. Curran Associates, Inc., 2019.
- [13] A. Nair, S. Bahl, A. Khazatsky, V. Pong, G. Berseth, and S. Levine, "Contextual imagined goals for self-supervised robotic learning," in *Proceedings of the Conference on Robot Learning*, ser. Proceedings of Machine Learning Research, L. P. Kaelbling, D. Kragic, and K. Sugiyama, Eds., vol. 100. PMLR, 30 Oct–01 Nov 2020, pp. 530–539. [Online]. Available: <https://proceedings.mlr.press/v100/nair20a.html>
- [14] Y. Wu, M. Mozifian, and F. Shkurti, "Shaping rewards for reinforcement learning with imperfect demonstrations using generative models," in *2021 IEEE International Conference on Robotics and Automation (ICRA)*, 2021, pp. 6628–6634.
- [15] Y. Seo, J. Kim, S. James, K. Lee, J. Shin, and P. Abbeel, "Multi-view masked world models for visual robotic manipulation," 2023.
- [16] M. Zhang, S. Vikram, L. Smith, P. Abbeel, M. Johnson, and S. Levine, "SOLAR: Deep structured representations for model-based reinforcement learning," in *Proceedings of the 36th International Conference on Machine Learning*, ser. Proceedings of Machine Learning Research, K. Chaudhuri and R. Salakhutdinov, Eds., vol. 97. PMLR, 09–15 Jun 2019, pp. 7444–7453. [Online]. Available: <https://proceedings.mlr.press/v97/zhang19m.html>
- [17] S. Ferraro, T. V. de Maele, T. Verbelen, and B. Dhoedt, "Symmetry and complexity in object-centric deep active inference models," *Interface Focus*, vol. 13, no. 3, apr 2023.
- [18] H. Shen, J. Yosinski, P. Kormushev, D. G. Caldwell, and H. Lipson, "Learning fast quadruped robot gaits with the rl power spline parameterization," *Cybernetics and Information Technologies*, vol. 12, no. 3, pp. 66–75, 2013. [Online]. Available: <https://doi.org/10.2478/cait-2012-0022>
- [19] A. L. Mitchell, M. Engelcke, O. P. Jones, D. Surovik, S. Gangapurwala, O. Melon, I. Havoutis, and I. Posner, "First steps: Latent-space control with semantic constraints for quadruped locomotion," in *2020 IEEE/RSJ International Conference on Intelligent Robots and Systems (IROS)*, 2020, pp. 5343–5350.
- [20] D. Kang, J. Cheng, M. Zamora, F. Zargarbashi, and S. Coros, "RI + model-based control: Using on-demand optimal control to learn versatile legged locomotion," 2023.
- [21] D. Hafner, T. P. Lillicrap, M. Norouzi, and J. Ba, "Mastering atari with discrete world models," *CoRR*, vol. abs/2010.02193, 2020. [Online]. Available: <https://arxiv.org/abs/2010.02193>
- [22] Mazzaglia, Pietro and Catal, Ozan and Verbelen, Tim and Dhoedt, Bart, "Curiosity-driven exploration via latent Bayesian surprise," in *PROCEEDINGS OF THE AAAI CONFERENCE ON ARTIFICIAL INTELLIGENCE*, Sycara, Katia and Honavar, Vasant and Spaan, Matthijs, Ed., vol. 36, no. 7. Association for the Advancement of Artificial Intelligence (AAAI), 2022, pp. 7752–7760. [Online]. Available: <http://dx.doi.org/10.1609/aaai.v36i7.20743>
- [23] M. Savva, A. Kadian, O. Maksymets, Y. Zhao, E. Wijmans, B. Jain, J. Straub, J. Liu, V. Koltun, J. Malik, D. Parikh, and D. Batra, "Habitat: A platform for embodied ai research," in *Proceedings of the IEEE/CVF International Conference on Computer Vision (ICCV)*, October 2019.
- [24] S. Parisi, V. Dean, D. Pathak, and A. Gupta, "Interesting object, curious agent: Learning task-agnostic exploration," in *Advances in Neural Information Processing Systems*, M. Ranzato, A. Beygelzimer, Y. Dauphin, P. Liang, and J. W. Vaughan, Eds., vol. 34. Curran Associates, Inc., 2021, pp. 20 516–20 530.
- [25] J. A. Placed, J. Strader, H. Carrillo, N. Atanasov, V. Indelman, L. Carlone, and J. A. Castellanos, "A survey on active simultaneous localization and mapping: State of the art and new frontiers," *IEEE Transactions on Robotics*, pp. 1–20, 2023.
- [26] F. Sadeghi and S. Levine, "Cad2rl: Real single-image flight without a single real image," *CoRR*, vol. abs/1611.04201, 2016. [Online]. Available: <http://arxiv.org/abs/1611.04201>
- [27] M. Müller, A. Dosovitskiy, B. Ghanem, and V. Koltun, "Driving policy transfer via modularity and abstraction," *CoRR*, vol. abs/1804.09364, 2018. [Online]. Available: <http://arxiv.org/abs/1804.09364>
- [28] J. Janai, F. Güney, A. Behl, and A. Geiger, "Computer vision for autonomous vehicles: Problems, datasets and state-of-the-art," *CoRR*, vol. abs/1704.05519, 2017. [Online]. Available: <http://arxiv.org/abs/1704.05519>
- [29] D. Feng, C. Haase-Schütz, L. Rosenbaum, H. Hertlein, F. Duffhaus, C. Gläser, W. Wiesbeck, and K. Dietmayer, "Deep multi-modal object detection and semantic segmentation for autonomous driving: Datasets, methods, and challenges," *CoRR*, vol. abs/1902.07830, 2019. [Online]. Available: <http://arxiv.org/abs/1902.07830>
- [30] D. Silver, J. A. Bagnell, and A. Stentz, "Learning from demonstration for autonomous navigation in complex unstructured terrain," *The International Journal of Robotics Research*, vol. 29, no. 12, pp. 1565–1592, 2010. [Online]. Available: <https://doi.org/10.1177/0278364910369715>
- [31] S. Gupta, J. Davidson, S. Levine, R. Sukthankar, and J. Malik, "Cognitive mapping and planning for visual navigation," *CoRR*, vol. abs/1702.03920, 2017. [Online]. Available: <http://arxiv.org/abs/1702.03920>
- [32] D. S. Chaplot, D. Gandhi, S. Gupta, A. Gupta, and R. Salakhutdinov, "Learning to explore using active neural SLAM," *CoRR*, vol. abs/2004.05155, 2020. [Online]. Available: <https://arxiv.org/abs/2004.05155>
- [33] D. Ha and J. Schmidhuber, "World models," *CoRR*, vol. abs/1803.10122, 2018. [Online]. Available: <http://arxiv.org/abs/1803.10122>
- [34] P. Wu, A. Escontrela, D. Hafner, K. Goldberg, and P. Abbeel, "Daydreamer: World models for physical robot learning," 2022.
- [35] D. Pathak, P. Agrawal, A. A. Efros, and T. Darrell, "Curiosity-driven exploration by self-supervised prediction," in *Proceedings of the 34th International Conference on Machine Learning - Volume 70*, ser. ICML'17, 2017, p. 2778–2787.
- [36] D. Yarats, R. Fergus, A. Lazaric, and L. Pinto, "Reinforcement learning with prototypical representations," 2021.
- [37] Y. Burda, H. Edwards, A. J. Storkey, and O. Klimov, "Exploration by random network distillation," *ICLR*, 2019.
- [38] R. Houthoofd, X. Chen, Y. Duan, J. Schulman, F. D. Turck, and P. Abbeel, "Vime: Variational information maximizing exploration," 2017.

- [39] J. Achiam and S. Sastry, "Surprise-based intrinsic motivation for deep reinforcement learning," 2017.
- [40] R. Sekar, O. Rybkin, K. Daniilidis, P. Abbeel, D. Hafner, and D. Pathak, "Planning to explore via self-supervised world models," in *ICML*, 2020.
- [41] S. Rajeswar, P. Mazzaglia, T. Verbelen, A. Piché, B. Dhoedt, A. Courville, and A. Lacoste, "Mastering the unsupervised reinforcement learning benchmark from pixels," in *40th International Conference on Machine Learning*, 2023. [Online]. Available: <https://arxiv.org/abs/2209.12016>
- [42] D. Hafner, T. Lillicrap, I. Fischer, R. Villegas, D. Ha, H. Lee, and J. Davidson, "Learning latent dynamics for planning from pixels," 2019.
- [43] Y. LeCun, P. Haffner, L. Bottou, and Y. Bengio, "Object recognition with gradient-based learning," in *Shape, contour and grouping in computer vision*. Springer, 1999, pp. 319–345.
- [44] F. E. Daum, *Extended Kalman Filters*. London: Springer London, 2015, pp. 411–413. [Online]. Available: https://doi.org/10.1007/978-1-4471-5058-9_62
- [45] J. Straub, T. Whelan, L. Ma, Y. Chen, E. Wijmans, S. Green, J. J. Engel, R. Mur-Artal, C. Ren, S. Verma, A. Clarkson, M. Yan, B. Budge, Y. Yan, X. Pan, J. Yon, Y. Zou, K. Leon, N. Carter, J. Briales, T. Gillingham, E. Mueggler, L. Pesqueira, M. Savva, D. Batra, H. M. Strasdat, R. D. Nardi, M. Goesele, S. Lovegrove, and R. A. Newcombe, "The replica dataset: A digital replica of indoor spaces," *CoRR*, vol. abs/1906.05797, 2019. [Online]. Available: <http://arxiv.org/abs/1906.05797>

APPENDIX

A. Model hyperparameters

Here, we report the hyperparameters for the world model, actor and critic networks, following the experimental setting of [21].

Name	Value
World Model	
Batch size	50
Batch sequence length	50
Discrete latent state dimension	32
Discrete latent classes	32
GRU cell dimension	200
KL free nats	1
KL balancing	0.8
Adam learning rate	$3 \cdot 10^{-4}$
Slow critic update interval	100
Actor-Critic	
Imagination horizon	15
γ parameter	0.99
λ parameter	0.95
Adam learning rate	$8 \cdot 10^{-5}$
Actor entropy loss scale	$1 \cdot 10^{-4}$
Common	
MLP number of layers	4
MLP number of units	400
Hidden layers dimension	400
Adam epsilon	$1 \cdot 10^{-5}$
Weight decay	$1 \cdot 10^{-6}$
Gradient clipping	100

TABLE I: World model, actor-critic and common hyperparameters.

B. Simulation

The simulated environments, namely apartment 0, apartment 1, and apartment 2, were sourced from the Replica-Dataset [45]. This dataset contains photo-realistic scenes used in our experiments.

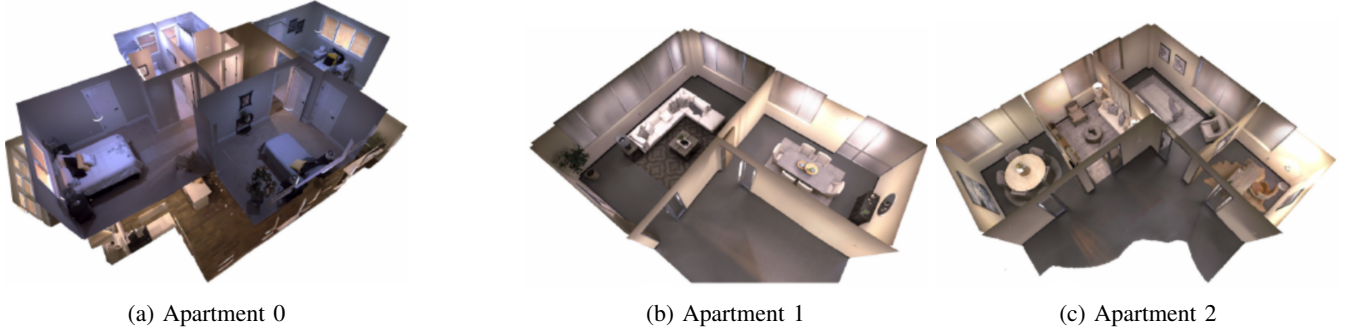


Fig. 5: Habitat simulation environments extracted from the Replica-Dataset

Those apartments are designed as real apartments, proposing large spaces to visit as is shown in Tab.II.

	apartement 0	apartement 1	apartement 2
surface	$58.69m^2$	$53.32m^2$	$45.31m^2$
visitable states	23476	21328	18123

TABLE II: Apartments number of visitable states (cells of 5 by 5 cm) and equivalent surface in m^2 .

C-BET, for which we adopt the open-source implementation (available at <https://github.com/sparisi/cbet>), underwent a training process following the protocol outlined in the study by [24], involving 5 million training steps. A

comparative analysis of the final exploration coverage after full training is presented in Fig.9, revealing that our model, trained for 2 million steps, achieved commendable coverage. Despite the extended training duration of 5 million steps, C-BET exhibited significantly lower exploration coverage in apartments 0 and 1. Apartment 2 exhibited comparable exploration between the two models. Notably, our model demonstrates a more efficient exploration strategy, while C-BET exhibited a tendency to revisit certain areas before venturing into new regions.

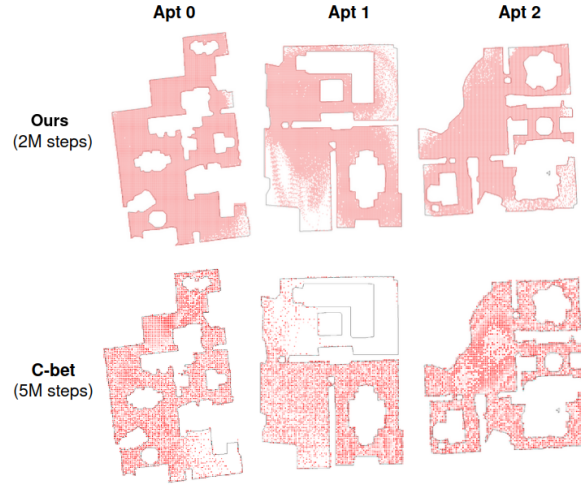


Fig. 6: Top view of the best heat-map coverage of the 3 apartments by ours and C-BET model after their attributed maximum number of steps.

C. Real world

The following section presents images providing visual insight into the real-world environments utilized for testing purposes. These pictures showcase the spaces where our navigation techniques were evaluated.



Fig. 7: Picture of the setup of the first real-world environment : "Small Real World".



(a) lab overall landscape



(b) utter left aisle of the lab



(c) center left aisle of the lab



(d) center right aisle of the lab



(e) utter right aisle of the lab

Fig. 8: Picture of the initial setup of the large real-world environment.

D. Auto docking

The agent is able to determine its own path to reach the docking station upon completion of its exploration or depletion of its battery. However, sometimes it failed and thus required human intervention to plug it back into its station manually. The main cause of not getting to the docking station is due to too much drift on the wheels of the robot, leading to a very inaccurate position estimation. In a small environment, the agent corrects its position upon docking; however, in a large environment, it leads to failure as it is not able to locate the docking station that is localized by the agent up to 1m from it.

	requests	success	success ratio
Small world auto docking	596	572	96%
Large world auto docking	1023	758	74%

TABLE III: Number of auto-docking request and success ratio in each environment.

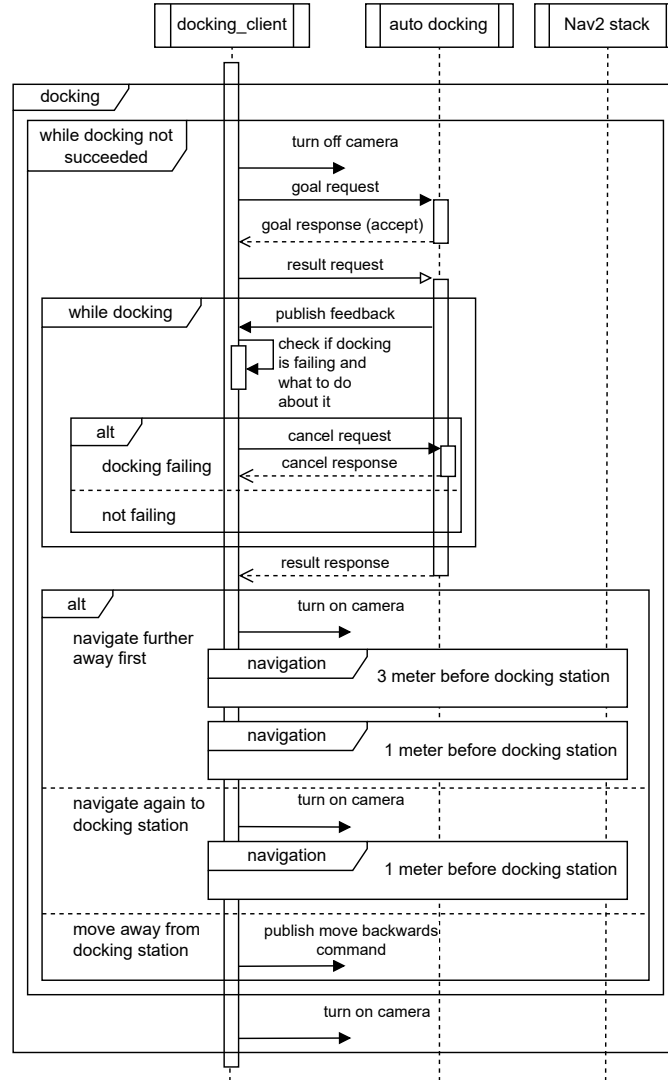


Fig. 9: The docking client node requests a docking goal to the auto docking action server. Recovery systems are used to make sure the docking process succeeds.